Dynamic Interactions of Fluorescence Probes with the Solvent Environment[1a]

Robert P. DeToma,[1b] J. Hamilton Easter,[1c] and Ludwig Brand*[1d]

Contribution No. 861 from the McCollum-Pratt Institute, Biology Department and McCollum-Pratt Institute, The Johns Hopkins University, Baltimore, Maryland 21218.
Received December 1, 1975

Abstract: Nanosecond time-resolved emission spectroscopy has been used to investigate the excited-state interaction between *N*-arylaminonaphthalene sulfonates and a model solvent, glycerol, as well as with the binding-site environment on egg lecithin vesicles. A dynamic interaction associated with a significant change in energy of the emission is observed on the nanosecond time scale. The results are consistent with a kinetic model for solvent relaxation. The decay kinetics as a function of wavelength are complex and are not consistent with the notion of only two emitting species changing in proportion during the dynamic approach to excited-state equilibrium. The excited-state reactions are described in terms of a wavelength-independent damping function, $i(t)$, and a dynamic spectral contour, $\rho(\bar{\nu},t)$, that shifts to low emission wavenumber ($\bar{\nu}$) with time. A comparison of the behavior in glycerol and with egg lecithin vesicles stresses the importance of kinetic effects on the fluorescence of probes when they are bound to biological materials.

Substituted naphthalene derivatives such as 1,8-ANS[2] and 2,6-*p*-TNS[2] have been extensively used as fluorescence probes to obtain information about proteins and membranes.[3,4] Weber and Laurence[5] first reported the dramatic observation that 1,8-ANS emits only weak green fluorescence in aqueous solution while intense blue fluorescence is observed when the dye is adsorbed to serum albumin. In solution the fluorescence of these probes depends on solvent polarity as well as on the temperature and viscosity. It is clear that the fluorescence emission depends on the character and rates of excited-state reactions. Stryer[6] was the first to propose that the dependence of the fluorescence emission maximum of 1,8-ANS on solvent polarity could be interpreted in terms of a dipole orientation mechanism. Additional studies[7-9] making use of steady-state fluorescence spectroscopy suggested that excited-state solvent relaxation might be a key process responsible for the sensitivity of the fluorescence of these dyes to the nature of the solvent. Spencer et al.[10] reported decay measurements of 1,8-ANS in propanol and 1,2-propanediol. Their observation that the decay time, measured in 1,2-propanediol, increases with increasing emission wavelength is consistent with an excited-state reaction on the nanosecond time scale.

Other proposals for the effect of solvent environment on the fluorescence of these probes have invoked more specific excited-state reactions. For example, steady-state luminescence as well as transient absorption spectroscopy led Kosower et al.[11] to propose that an intramolecular excited-state charge-transfer reaction might have a key role. A significant feature of this mechanism is the existence of a two-state excited-state reaction involving two distinct emitting species.

While steady-state fluorescence spectra reflect energetic transitions that occur prior to emission of light, additional information can be obtained by direct observation of the fluorescence spectra as a function of decay time.[12-16] A previous report[17] has described an instrumental and computational procedure for obtaining *deconvolved* nanosecond time-resolved emission spectra. The aim of the present paper is to describe results obtained by this technique with 2,6-*p*-TNS[2] and 2,6-ANS[2] in glycerol and with 2,6-*p*-TNS[2] adsorbed to egg lecithin vesicles (a model for a biological membrane). The results are analyzed according to a theory for solvent relaxation due to Bakhshiev et al.[18]

The effect of universal solvent interaction on absorption and fluorescence spectra has been treated by Lippert,[19] Mataga et al.,[20] Bakhshiev,[21] and others.[22,23] These authors have obtained theoretical or semiempirical expressions which relate the macroscopic dielectric properties of the solvent and chromophore to observed spectral shifts in the fluorescence and absorption spectra.

For a descriptive view of the time evolution of spectral shifts due to universal solvent-excited solute interactions, it is useful to invoke the Franck–Condon principle. Upon excitation a molecule will retain the particular solvent configuration which is favored by the ground state, since solvent molecules cannot reorient during the excitation process. If the excited state that was formed directly through light absorption (or indirectly in a fast subnanosecond reaction) has a new dipole moment, and if the solvent reorientation time is less than the fluorescence lifetime, the solvent dielectric medium surrounding the dye will be polarized differently than in the ground state. Thus a new reaction field developed by this orientation strain is created and the solvent molecules will reorient (relax) to accommodate the change in dipole moment of the excited solute molecule until solvation equilibrium has been restored. When the solvent relaxation time is comparable to the fluorescence lifetime, time-resolved spectral shifts in addition to electronic relaxation will be observable on the nanosecond time scale.

The phenomenon described here represents the photostationary fluorescence spectrum as a superposition of the elementary time-dependent spectra which evolve from an initially formed Franck–Condon spectrum (vibrationally relaxed) that is being damped electronically and that is continuously shifting in time to low energy in accordance with universal dipolar solvent interaction. Mazurenko and Bakhshiev[24] have formally expressed the nonexponential decay law which governs this process as[25]

$$I(\bar{\nu},t) = i(t)\rho(\bar{\nu} - \xi(t)) \qquad (1)$$

where $i(t)$ is a damping term which would characterize the decay law of the excited molecular system in the absence of spectral shifts, and $\rho(\bar{\nu} - \xi(t))$ represents the normalized quantum intensity distribution in the elementary spectrum shifted in energy by the amount $\xi(t)$ at time t. Although $I(\bar{\nu},t)$ kinetically represents a continuous distribution of relaxing states, according to the formulation of eq 1 a complex system of this type can be considered as a singly excited species with a characteristic wavelength-independent decay law, $i(t)$, and with a spectrum which is continuously shifting in time. Equation 1 states that knowing the contour of an elementary spectrum at any one time and the undistorted damping term, $i(t)$, the complete time-resolved intensity surface can be uniquely characterized by a position parameter $\xi(t)$. $\xi(t)$ describes the spectral relaxation kinetics of the solvent reorientation process. The decay parameter(s) associated with $\xi(t)$

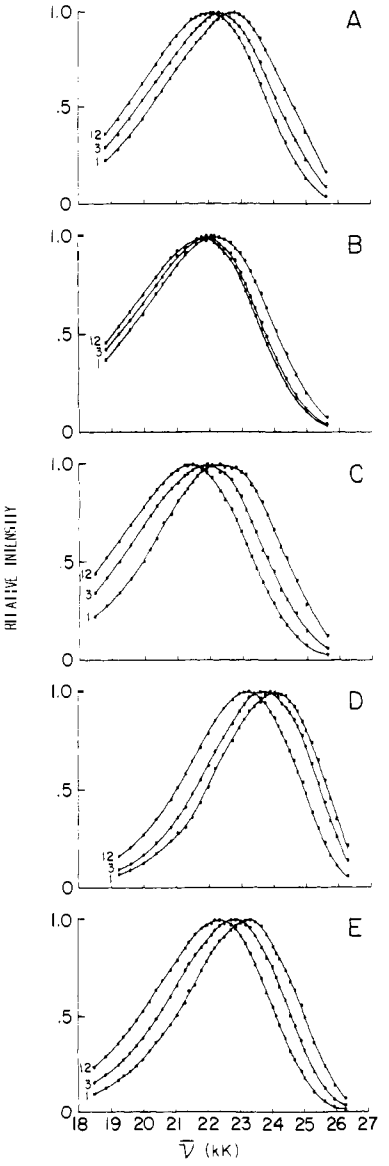

Figure 1. Deconvolved nanosecond time-resolved fluorescence spectra shown at 1, 3, and 12 ns after photoexcitation for TNS–vesicle at 7 °C (A) and at 32 °C (B), for TNS–glycerol at 10 °C (C), and for ANS–glycerol at −10 °C (D) and at 10 °C (E). These spectra have been peak normalized.

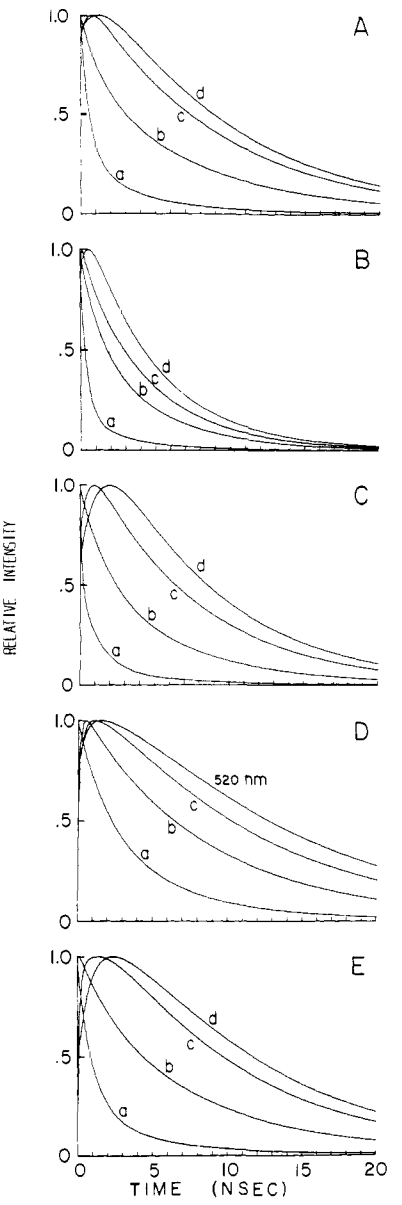

Figure 2. Normalized fluorescence impulse response functions generated from empirical deconvolution parameters for the system TNS–vesicle at 7 °C (A) and at 32 °C (B), TNS–glycerol at 10 °C (C), and ANS–glycerol at −10 °C (D) and at 10 °C (E): (a) 390 nm, (b) 435 nm, (c) 485 nm, (d) 530 nm.

can be related to the dielectric properties of the solvent and solute.[24,26]

The overall decay kinetics according to eq 1 reflect contributions due to electronic relaxation and spectral relaxation. In this paper time-resolved emission spectral data are reduced according to the ideas presented above. The electronic relaxation component, $i(t)$, is empirically characterized and the spectral relaxation data $\xi(t)$ and $\rho(\bar{\nu} - \xi(t))$ are presented.

Experimental Section

TNS[2] and ANS[2] (sodium salts) were prepared by Seliskar.[9] Egg lecithin vesicles were prepared as previously described.[27] The TNS–vesicle complex used in these measurements was characterized by TNS (11 μM) and lecithin (0.86 mM). Anhydrous spectral grade glycerol (for fluorescence microscopy; E. Merck Darmstadt) was used to prepare the ANS and TNS solutions (ca. 5×10^{-6} M). These solutions were thoroughly mixed under vacuum and were handled under vacuum or in an argon atmosphere. The glycerol solutions were stored in the dark and were protected from moisture contamination.

The instrumentation and computational procedures used for the generation of deconvolved nanosecond time-resolved emission spectra have been described in detail elsewhere.[17] Fluorescence decay curves were collected by the single-photon counting method at selected emission wavelengths throughout the fluorescence spectrum (typically 30–40 wavelengths were chosen). Each decay curve and excitation profile were collected in a semisimultaneous mode by use of a turntable stepper-motor (under computer control) in order to minimize long-term timing variations in the excitation profile. Time-resolved emission spectra were generated from impulse response functions obtained by empirical deconvolution of the fluorescence decay curves. Empirical deconvolution was achieved by nonlinear regression analysis based on a multiexponential impulse model. Under the excitation conditions (337 nm) of these experiments no measurable photodecomposition was detected for any of the samples employed.

Results

Time-Resolved Spectral Properties. Deconvolved nanosecond time-resolved emission spectra (TRES) were obtained for the following systems: 2-*p*-toluidinonaphthalene 6-sulfonate adsorbed to lecithin vesicles (TNS–vesicles) at 7 and 32 °C, TNS dissolved in glycerol (TNS–glycerol) at 10 °C, and 2-anilinonaphthalene 6-sulfonate dissolved in glycerol (ANS–glycerol) at 10 and −10 °C. These spectra are shown in Figure

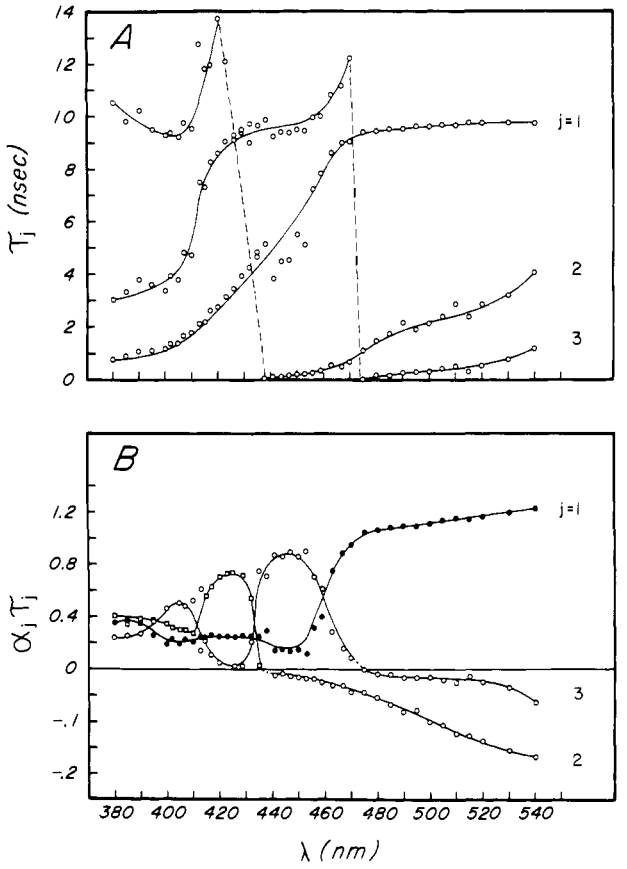

Figure 3. A. Decay times vs. emission wavelength (λ) for a three-exponential $[f(\lambda,t) = \Sigma_{j=1}^{3}\alpha_j(\lambda)e^{-t/\tau_j(\lambda)}]$ empirical deconvolution of the time-resolved fluorescence decay data for the system ANS-glycerol at 10 °C. B. The product of each α_j and τ_j pair obtained from the empirical deconvolution described in A normalized to constant emission intensity $\Sigma_{j=1}^{3}\alpha_j\tau_j = 1$ shown as a function of λ for the same exponential component ordering (j) in A. This plot illustrates the relative exponential component contribution to the total fluorescence at each λ.

1 at three representative times.[28] In each case a continuous shift of the emission spectra to low energy is observed with increasing time. The rate and magnitude of this shift depend on the temperature, the environment of the dye, and the nature of the dye. In addition, it is seen that the band shape of these spectra shows little or no variation with time.

Figure 2 shows the fluorescence impulse response functions obtained at four different wavelengths with the systems described above. In every case the mean decay time increases with increasing wavelength and at the red tail of the emission spectrum (e.g., >480 nm) the intensity builds up from a low value at time zero to a maximum and then decays. This latter behavior demonstrates that a portion of the light emitted at the red end of the spectrum results from an excited-state reaction. The experimental impulse decay curves shown here bear a striking resemblance to theoretical decay curves predicted by Bakhshiev et al.[18] for an excited molecular system undergoing universal excited-state solvent relaxation.

Empirical deconvolution of the raw fluorescence decay data revealed complex decay kinetics in all cases studied. These data required a minimum of three exponential terms to give an acceptable fit and the decay times obtained varied with emission wavelength. The empirical decay parameters for one of the systems studied (ANS-glycerol at 10°) are plotted in Figure 3 as a function of wavelength to illustrate the complex nature of the photokinetics in these systems. The decay parameters in these plots were derived from a typical deconvolution based on a three-exponential impulse model,[29] $f(\lambda,t) = \alpha_1(\lambda)e^{-t/\tau_1(\lambda)} + \alpha_2(\lambda)e^{-t/\tau_2(\lambda)} + \alpha_3(\lambda)e^{-t/\tau_3(\lambda)}$. These results obtained with

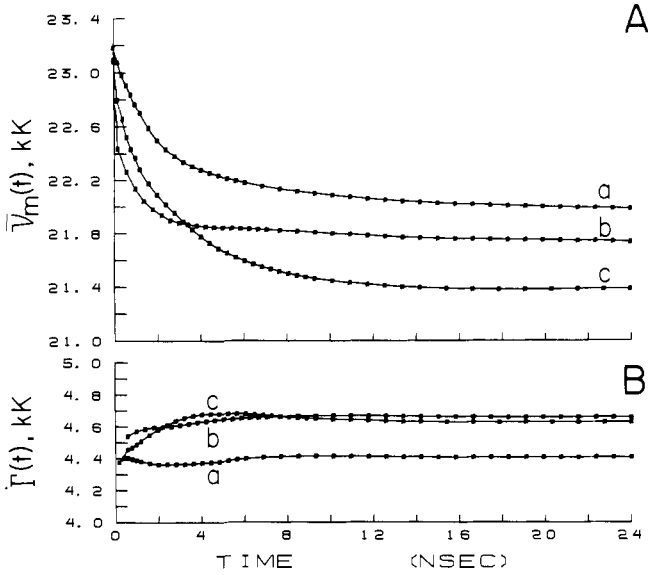

Figure 4. A. Emission maxima (spectral position) vs. time for TNS-vesicle at 7 °C (a) and 32 °C (b) and TNS-glycerol at 10 °C (c). B. Bandwidth vs. time for the systems a,b,c as designated in A.

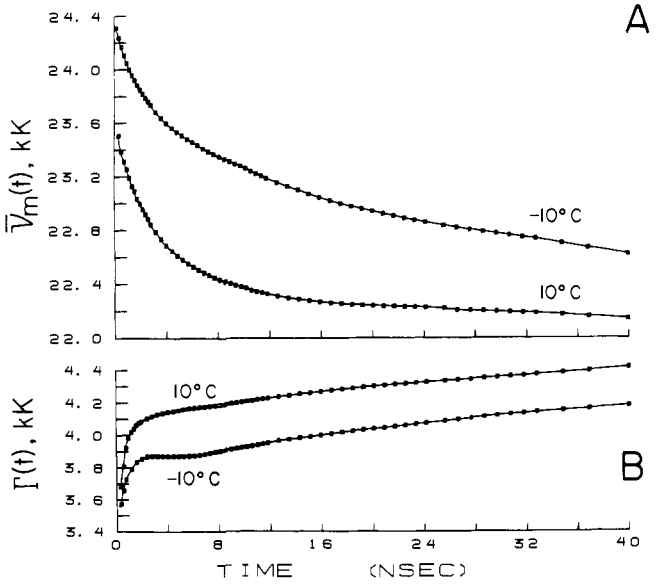

Figure 5. A. Emission maxima (spectral position) vs. time for ANS dissolved in glycerol at two temperatures. B. Bandwidth vs. time for the ANS system described in A.

TNS and ANS in several solvent environments are not consistent with a simple two-state relaxation model or with any solvent interaction model that features two emitting states as distinct chemical species. Such a model would predict a single or double exponential decay over the entire emission spectrum with decay times invariant with emission wavelength. The observed photokinetics are complex and appear to be nonexponential.

The time-dependent spectral shifts such as those indicated in Figure 1 are better represented by the plots shown in Figures 4 A and 5 A. Here the spectral positions as characterized by the wavenumber at maximum emission intensity $[\xi(t) = \bar{\nu}_m(t)]$ are plotted as a function of time. Such plots describe the kinetics of the observed spectral relaxation subsequent to photoexcitation with a δ-function light pulse. The dependence of the rate of spectral relaxation on temperature is apparent. In Figure 4 A an increase in the temperature from 7 to 32 °C for the TNS-vescile system is shown to result in a substantial in-

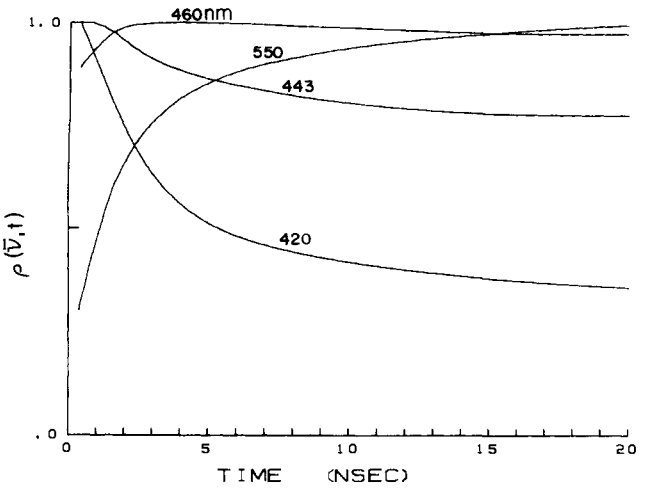

Figure 6. Emission energy shift functions, $\rho(\bar{\nu},t)$, plotted against time and shown at four wavelengths for TNS dissolved in glycerol at 10 °C. These functions are presented normalized at their maximum values.

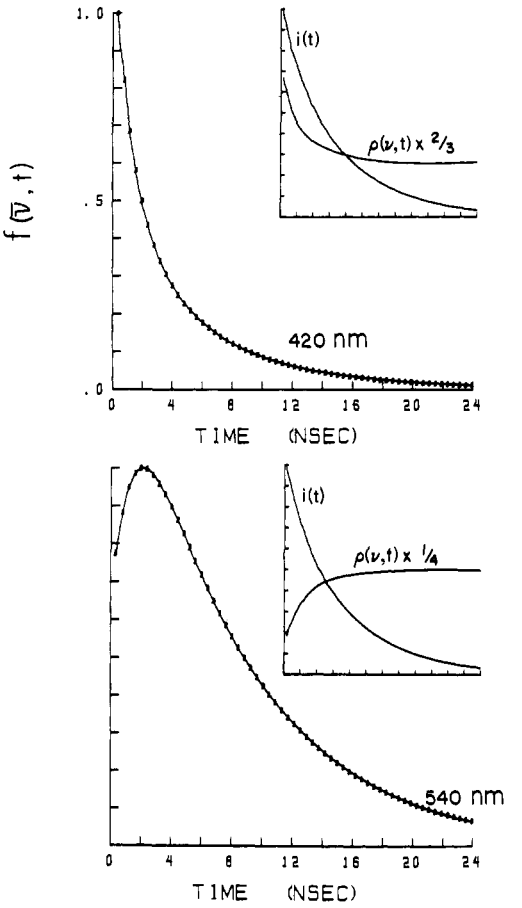

Figure 7. Typical fits at two emission wavelengths (λ) of the experimental impulse decay curves (■) to the Bakhshiev model (eq 2, text) for TNS in glycerol at 10 °C. The solid lines superimposed on these data points are the calculated fits. The common $i(t)$ at each λ is represented in the upper inserts along with the λ-characteristic shift functions, $\rho(\bar{\nu},t)$.

crease in the rate of spectral relaxation. The ANS-glycerol system (Figure 5 A) shows a qualitatively similar dependence for a 20 °C temperature differential. In comparing TNS with ANS in glycerol at the same temperature, it is observed that the absolute spectral position differs considerably; however, the interaction energy associated with this relaxation process is similar, ~1.6 kK for the two dyes. The comparison of TNS-vesicles with TNS-glycerol at similar temperatures of 7 and 10°, respectively, shows that the absolute spectral position, the interaction energy, and rate of spectral shift differ significantly in these systems. Analysis of this spectral relaxation data in terms of the function $[\bar{\nu}_m(t) - \bar{\nu}_m(\infty)]$ employing a suitable value for the relaxed spectral position, $\bar{\nu}_m(\infty)$, where appropriate, revealed that the kinetics describing these red shifts were not monoexponential as suggested by Mazurenko.[26] A minimum of two well-separated relaxation times were involved (e.g., the TNS-vesicle system at 7 °C yielded relaxation times of 1.5 and 7.1 ns in the proportion of 1:0.61, respectively). Before any attempt is made to describe the spectral kinetics of these systems by dielectric relaxation theory involving several exponential relaxation times,[26] careful attention must be given to considering contributions from specific solvent interactions as a possible explanation for the observed behavior.

The band shape of the time-resolved emission spectra may be characterized by Γ, the full width at half-maximum bandwidth. The time-dependent bandwidth data for the TNS-vesicle and the TNS-glycerol systems are shown in Figure 4 B. Each system eventually attains a steady bandwidth with time. Minor variations in bandwidth are observed with the TNS-vesicle system at 32 °C and with the TNS-glycerol system at 10 °C. These amount to a maximum change of not more than 6% which is observed in the time period between 0 and 9 ns.[30]

The bandwidth plots for the ANS-glycerol system at two temperatures are shown in Figure 5 B. In contrast to the results with TNS, a constant-value bandwidth is not reached within the first 40 ns. There is a small but steady increase in bandwidth (~7% referenced to the mean value at ~20 ns) between 3 and 40 ns. An additional rapid change in bandwidth occurs during the first 3 ns.[30]

The salient features of these data indicate that in the TNS system the time-resolved spectral bandwidth remains essentially constant whereas in the ANS system the change in Γ is small but apparently significant due to the steady variation that is observed throughout the entire temporal range examined. In addition, a modest temperature dependence of the time-resolved bandwidth is observed in Figures 4 B and 5 B for the TNS-vesicle and ANS-glycerol systems.

Analysis in Terms of the Bakhshiev Formulation. In describing the overall kinetic behavior of the solvent relaxation process, eq 1 may be rewritten in a more implicit notation

$$I(\bar{\nu},t) = i(t)\rho(\bar{\nu},t) \qquad (2)$$

The special features of representing $I(\bar{\nu},t)$[25] in this manner which distinguish a continuous solvent relaxation process from a stationary multi-state (two- or three-state) system are the following. (i) Ideally, when the band shape of the spectral contour, $\rho(\bar{\nu},t)$, remains invariant with time, strong evidence is provided in support of the solvent relaxation process. In fact, eq 2 in its present form can be rigorously applied as a kinetic model for solvent relaxation only when a band shape variation with time is small or absent. (ii) In a stationary system the decay kinetics are described by a multiexponential decay law with decay times invariant with emission wavelength. The damping function for such a system when obtained in the manner to be described [normalization of $I(\bar{\nu},t)$ to constant quanta] will retain these same characteristic decay times. The decay kinetics according to eq 2 for a system undergoing solvent relaxation, however, are nonexponential and when empirically fitted to a multiexponential model will yield wavelength-dependent decay times. Since $i(t)$ is defined as being wavelength-independent, a one-to-one correspondence between the decay times in $i(t)$ and $I(\bar{\nu},t)$ cannot be possible. (iii) For a photoexcited molecular system undergoing solvent relaxation, obtaining $i(t)$ determines a new important parameter of the

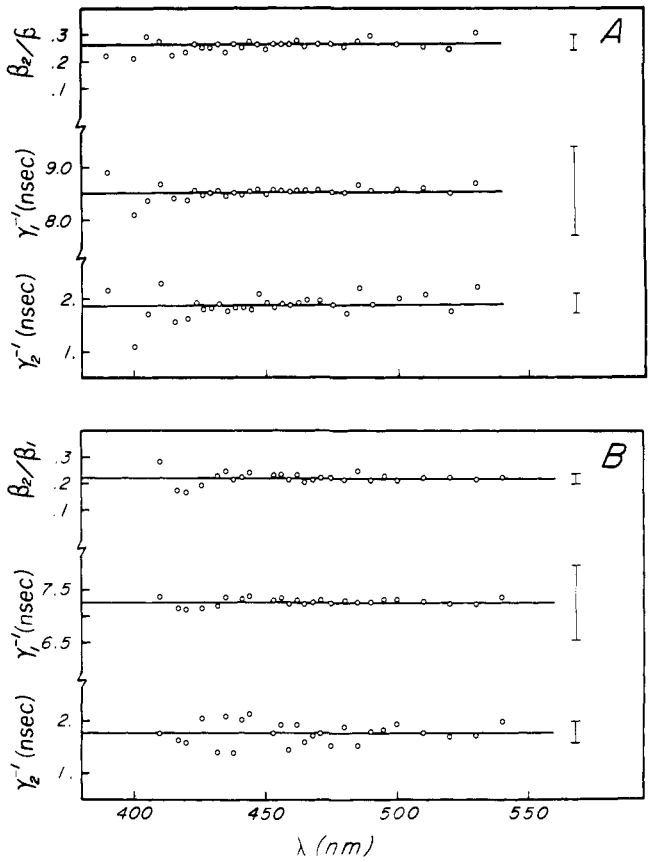

Figure 8. Recovered biexponential damping parameters (O) vs. emission wavelength for TNS-vesicles at 7 °C (A) and TNS-glycerol at 10 °C (B). Vertical bars (I) indicate ±10% error limits about mean values of the parameters which are represented by the solid lines (see eq 4 in text).

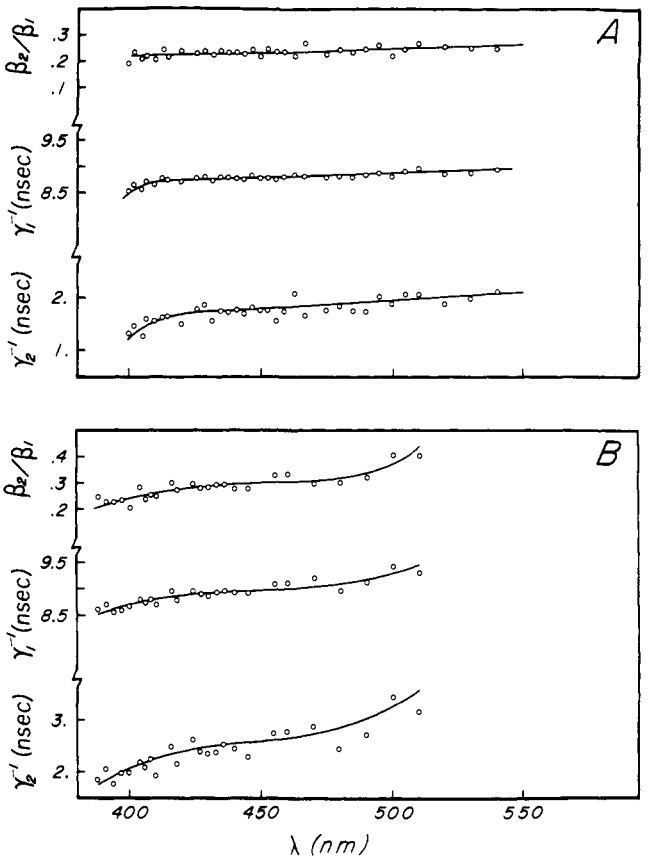

Figure 9. Recovered biexponential damping parameters (O) vs. emission wavelength for ANS-glycerol at 10 °C (A) and at −10 °C (B) (see eq 4 in text).

system, whereas in a stationary system the formulation of eq 2 is unnecessary and nothing new is learned.

Since the quantity $\rho(\bar{\nu},t)$ when considered a function of $\bar{\nu}$ at fixed t actually represents the normalized quantum intensity distribution in an elementary spectrum of the TRES, the damping function, $i(t)$, can be readily determined. $\rho(\bar{\nu},t)$ is first obtained as a function of t at each $\bar{\nu}$ by normalizing each time slice of the complete surface $I(\bar{\nu},t)$ to constant emitted quanta and extracting the numeric values of $\rho(\bar{\nu},t)$ at each $\bar{\nu}$.[31] Knowing $\rho(\bar{\nu},t)$ and the fluorescence impulse functions, $I(\bar{\nu},t)$ [or $f(\bar{\nu},t)$],[25] at each $\bar{\nu}$ as a function of time determines $i(t)$, which should be independent of $\bar{\nu}$.

Representative plots of $\rho(\bar{\nu},t)$ as a function of time for several emission wavelengths are shown in Figure 6 for the TNS-glycerol system at 10 °C. $\rho(\bar{\nu},t)$ is a complex function which depends on the kinetics of the spectral shift and the emission contour of the system. The change in $\rho(\bar{\nu},t)$ from a decreasing to an increasing function of time across the emission band from higher to lower energy is apparent and accounts for the characteristic increase in the mean decay time $[\int_0^\infty t \cdot f(\bar{\nu},t)dt / \int_0^\infty f(\bar{\nu},t)dt]$ with wavelength that is shown in Figure 2.

Nonlinear multiple regression analysis was used to obtain the damping function, $i(t)$, to within a scale factor at each $\bar{\nu}$ from $\rho(\bar{\nu},t)$ and $f(\bar{\nu},t)$[25] according to eq 2. The fitting function assumed that $i(t)$ could be expressed as a sum of exponentials.

$$i(t) = \sum_j \beta_j e^{-\gamma_j t} \tag{3}$$

The typical quality of recovery from this computation is shown in Figure 7 for the TNS-glycerol system at 10 °C. The observed fluorescence impulse curves at 420 and 540 nm are denoted by the points on these graphs. The product of $i(t) \times \rho(\bar{\nu},t)$, each shown separately in the upper right inserts, generates the solid line fits through the experimental data.

The damping function, $i(t)$, was recovered as a sum of two exponentials for all five systems investigated

$$i(t) = \beta_1 e^{-\gamma_1 t} + \beta_2 e^{-\gamma_2 t} \tag{4}$$

with the dominant contribution coming from the long decay time γ_1^{-1}. The parameters γ_1^{-1}, γ_2^{-1}, and β_2/β_1 are plotted as a function of emission wavelength in Figure 8 for TNS-glycerol and TNS-vesicles at 7 °C and in Figure 9 for the ANS-glycerol system at two temperatures.

Within the experimental scatter of the data, $i(t)$ is found to be independent of emission wavelength for the TNS systems. The results for TNS-vesicles at 32 °C which are not illustrated are 4.8 ns, 1.7 ns, and 0.33 for γ_1^{-1}, γ_2^{-1}, and β_2/β_1, respectively. The observed wavelength-independent nature of $i(t)$ confirms the peak normalization procedure for obtaining $\rho(\bar{\nu},t)$[31] which in turn marks eq 2 as a consistent model for describing the TNS-glycerol and TNS-vesicle decay kinetics.

For ANS dissolved in glycerol the damping function reflects a moderate dependence on emission wavelength which is particularly noticeable in the low-temperature data shown in Figure 9. This dependence on wavelength must be ascribed to the small but steady time-dependent band-shape changes (~0.25 kK) that were observed in this system which of necessity cause a failure of eq 2 in its present form to accurately represent such data. Note, however, that the discrepancies here are not dramatic and that the decay data for ANS-glycerol are reasonably approximated by eq 2. The analysis in terms of the Bakhshiev equation employing a peak normalization to

determine $\rho(\bar{\nu},t)$[31] provides a particularly sensitive test of decay data which reflects a continuous solvent relaxation process as is verified by the deviations detected here as well as by simulation experiments. These deviations direct attention to the possibility of specific interaction in combination with the universal solvent interaction that is presumably operative in this system.

The strong temperature dependence of $i(t)$ as reflected in the γ_1 decay parameter for TNS–vesicles as compared to the weak temperature dependence observed for ANS dissolved in glycerol should be noted. Apparently, the temperature dependence in ANS–glycerol is predominantly associated with the spectral relaxation kinetics of this system (Figure 5), whereas in the TNS–vesicle system both spectral and electronic relaxation are influenced by temperature over the narrow range examined.

It is emphasized that the functional form that was chosen to model the damping function (eq 3) and the resultant observable representation as a sum of two exponentials (eq 4) does not necessarily represent the mathematical form of the physical decay law for $i(t)$. Although excellent fits are obtained, the apparent biexponential nature of $i(t)$ can, at present, only provide a convenient way to analytically express this time dependence. The mathematical form of the actual physical decay law can only be deduced by further study. The significant point to be emphasized here is the fact that a complex kinetic process reflected by the wavelength dependence of the empirical decay parameters can be represented as the product of a wavelength-independent electronic damping function and a spectral contour that only shifts in time. These characteristics which describe universal dipolar solvent relaxation were experimentally verified in the TNS systems and were found approximately true in the ANS–glycerol system.

Discussion

Some general conclusions can be drawn from the time-resolved spectral studies presented in this paper for the TNS–vesicle, TNS–glycerol, and ANS–glycerol systems. (i) The observed time-resolved spectral shifts are associated with excited-state reactions on the nanosecond time scale. (ii) The inability to time resolve two or more distinct spectral components (with a 6.6-nm emission bandpass) in any of the systems studied, coupled with the observed complex decay kinetics, demonstrates that the spectral shifts occurring in the time window bounded by the fluorescence decay of the excited system and the time resolution of the decay instrument (~0.5 ns) cannot be solely explained by a mechanism involving only one or two distinct emitting species (states). (iii) The observed complex decay kinetics can be explained by a *dominant* mechanism based on universal solvent–excited solute interaction (solvent relaxation) as phenomenologically expressed by Bakhshiev. With regard to the work in glycerol these conclusions are not consistent with a simple one-state (or discrete two-state) assignment of excited ANS or TNS in this solvent at room temperature.[11,32]

For a dilute solution of dye free from impurities and excited by low levels of light the damping function, $i(t)$, of eq 2 is expected to be described by a single exponential decay with a total rate parameter, γ, containing a molecular fluorescence and an internal quenching component. It therefore remains necessary to explain the apparent biexponential damping function for the TNS and ANS systems, as well as the steady band-shape change that was observed only in the ANS–glycerol system, and thus to define the nature of the "excited solute" in these systems. In addition, the nature of the "solvent" in the TNS–vesicle system must ultimately be defined. The experiments presented here cannot in themselves provide these detailed answers; however, they do provide a sound basis for considering solvent relaxation as a key process in explaining the solvent-sensitive fluorescence properties of 2,6-*p*-TNS and 2,6-ANS.

The expectation that $i(t)$ describes a single exponential response assumes that the excited molecule, prior to solvent relaxation, represents a single excited state and does not internally interact to become a new excited species. It also assumes that the pure solvent does not represent itself as an "impurity" to the ground or excited state of the dye (specific solvent interaction). In addition, if the decay parameter, γ, depends on time either by way of a time-dependent quantum yield change in the spectrally relaxing system or through a transient evolution of concentration gradients with reference to a specific solvent-excited solute exciplex interaction, then the damping function will exhibit an apparent nonmonoexponential time dependence.[33]

Apart from the apparent biexponential damping function several other aspects of this study suggest that in addition to general solvent interaction, specific interactions may also be partly responsible for the observed behavior. As just indicated these could include specific intermolecular interactions with the solvent[34–36] as well as intramolecular interactions[11,37] which in a very rapid reaction prepare precursor states (species) capable of being stabilized by the solvent in a slower solvent reorientation process.

The early-time bandwidth variations that are observed with TNS and ANS in addition to the continuous band-shape change with time observed in the ANS data are consistent with specific interactions. The increase in time-resolved bandwidth with temperature in a given system suggests that the "excited solute" is formed in a rapid temperature-dependent reaction or that it evolves from a temperature-dependent ground-state association.

The rapid initial decay of the spectral relaxation data (Figures 4 and 5) represents a relatively large energetic interaction at early times. This behavior can be interpreted as the spectral shift one would associate with some specific interaction. An argument of this type has been used previously by Ware et al.[12] in support of specific exciplex interaction in the aminophthalimide–2-propanol system. However, such behavior cannot be used as a sole diagnostic to define specific interaction since dielectric continuum theory can account for complex spectral kinetics.[26]

With reference to specific solvent–solute interaction it is interesting that several studies indicate that associating solvents capable of hydrogen bonding interaction appear to show a strong effect.[36,38–40]

Based on the time-resolved fluorescence behavior of TNS and ANS dissolved in glycerol and previous studies,[36,38,39] we propose that the "excited solute" is prepared in a specific interaction on a time scale somewhat less (or perhaps slightly overlapping) the solvent reorientation time. Solvent relaxation around this "excited solute" then dominates the nanosecond time window. In order to detail this mechanism and thus to partition general solvation from specific interaction (and to define the nature of this specific interaction), further study in both viscous and fluid solution is required.

In fluid solutions solvent relaxation will be rapid and fluorescence will reflect the energetics of the final equilibrium state. The work described in this report represents a direct kinetic study of the approach to an excited-state equilibrium $[\bar{\nu}_m(\infty)]$. In viscous solutions such as glycerol, emission will occur before equilibrium has been achieved and this spectral kinetic effect will be significant. It is emphasized that when these dyes are adsorbed to biological materials such as lecithin vesicles as shown here, or to proteins as will be shown in a subsequent report, they behave as they do in glycerol with the spectral kinetic effect influencing the fluorescence.

In this work it was found that the time-resolved spectral behavior of TNS when adsorbed to vesicles, and of TNS and ANS when dissolved in a viscous solvent such as glycerol, could be adequately explained by a continuous "solvent" relaxation process on the nanosecond time scale (Bakhshiev model, eq 2).

For the vesicle data this observation represents a significant finding in that both the spectral and electronic relaxation components which are conveniently partitioned in this model reflect the probe-site interaction and on this level provide a means of correlating rate parameters contained in $i(t)$ and $\xi(t)$ with various perturbations on the probe-site environment. Nanosecond fluorescence techniques are capable of distinguishing various excited-state interactions with neighboring molecules such as exciplex formation, energy transfer, and general solvation. The use of nanosecond time-resolved emission spectroscopy in fluorescence probe studies with biological systems should provide for the possibility of a more detailed understanding of the probe environment, e.g., mobility and nature of interacting residues. In particular, the quantitative evaluation of the vesicle data in terms of the kinetic theory of dipolar solvent relaxation, as reported here, suggests the potential value of these probes to signal dipolar motion in the environment of the dye when bound to biological materials.

Acknowledgment. The authors thank Dr. Robert E. Dale for helpful discussion and advice.

References and Notes

(1) (a) This research was supported in part by NIH Grant No. GM11632; (b) supported by NIH Postdoctoral Fellowship No. 1F32 GM01268; (c) supported by NIH Training Grant No. GM-5T01-G57; (d) supported by NIH Career Award Development Grant No. GM10245.

(2) 1,8-ANS stands for 1-anilinonaphthalene 8-sulfonate and 2,6-*p*-TNS is an abbreviation for 2-*p*-toluidinonaphthalene 6-sulfonate. The naphthalene sulfonate derivatives used in the present study are 2,6-*p*-TNS and 2,6-ANS which will be denoted TNS and ANS, respectively.

(3) G. M. Edelman and W. O. McClure, *Acc. Chem. Res.*, **1**, 65 (1968).

(4) L. Brand and J. R. Gohlke, *Annu. Rev. Biochem.*, **41**, 843 (1972).

(5) G. Weber and D. J. R. Laurence, *Proc. Biochem. J.*, **56**, 31 (1954).

(6) L. Stryer, *J. Mol. Biol.*, **13**, 482 (1965).

(7) W. O. McClure and G. M. Edelman, *Biochemistry*, **5**, 1908 (1966).

(8) D. C. Turner and L. Brand, *Biochemistry*, **7**, 3381 (1968).

(9) C. J. Seliskar and L. Brand, *J. Am. Chem. Soc.*, **93**, 5405, 5414 (1971).

(10) R. D. Spencer, W. M. Vaughan, and G. Weber in "Molecular Luminescence", E. C. Lim, Ed., W. A. Benjamin, New York, N.Y., 1969, pp 607–629.

(11) E. M. Kosower, H. Dodiuk, K. Tanizawa, M. Ottolenghi, and N. Orbach, *J. Am. Chem. Soc.*, **97**, 2167 (1975).

(12) W. R. Ware, S. K. Lee, G. J. Brant, and P. P. Chow, *J. Chem. Phys.*, **54**, 4729 (1971).

(13) S. K. Chakrabarti and W. R. Ware, *J. Chem. Phys.*, **55**, 5494 (1971).

(14) N. Nakashima, H. Inoue, N. Mataga, and C. Yamanaka, *Bull. Chem. Soc. Jpn.*, **46**, 2288 (1973).

(15) K. Egawa, N. Nakashima, N. Mataga, and C. Yamanaka, *Bull. Chem. Soc. Jpn.*, **44**, 3287 (1971).

(16) L. Brand and J. R. Gohlke, *J. Biol. Chem.*, **246**, 2317 (1971).

(17) J. H. Easter, R. P. DeToma, and L. Brand, *Biophys. J.*, **16**, 571 (1976).

(18) N. G. Bakhshiev, Y. T. Mazurenko, and I. V. Piterskaya, *Opt. Spectrosc. (USSR)*, **21**, 307 (1966).

(19) E. Lippert, *Z. Electrochem.*, **61**, 962 (1957).

(20) N. Mataga, Y. Kaitu, and M. Koizumi, *Bull. Chem. Soc. Jpn.*, **29**, 465 (1956).

(21) N. G. Bakhshiev, *Opt. Spectrosc. (USSR)*, **7**, 29 (1959).

(22) M. F. Nicol, *Appl. Spectrosc. Rev.*, **8**, 183 (1974).

(23) N. Mataga and T. Kubata, "Molecular Interactions and Electronic Spectra", Marcel Dekker, New York, N.Y., 1970, p 371.

(24) Y. T. Mazurenko and N. G. Bakhshiev, *Opt. Spectrosc. (USSR)*, **28**, 490 (1970).

(25) $I(\bar{\nu},t)$ is the spectral-intensity normalized impulse response. It is related to the raw impulse response, $f(\bar{\nu},t)$, by a normalization factor, $h(\bar{\nu})$, which is obtained from the steady-state emission spectrum, i.e., $I(\bar{\nu},t) = h(\bar{\nu})\, f(\bar{\nu},t)$.[17]

(26) Y. T. Mazurenko, *Opt. Spectrosc. (USSR)*, **34**, 527 (1973).

(27) J. H. Easter and L. Brand, *Biochem. Biophys. Res. Commun.*, **52**, 1086 (1973).

(28) Although a high density of data along the $I(\bar{\nu},t)$ surface was actually obtained as previously described,[17] TRES are shown here at only three times for clarity of presentation. As will be shown, this high data density is necessary for a proper characterization of the time-resolved spectral properties.

(29) It should be emphasized that the impulse responses shown in Figure 2 and the TRES shown in Figure 1 obtained by empirical deconvolution required three or four exponential terms to obtain the desired "best fits". The best three exponential decay parameters are shown in Figure 3.

(30) The bandwidth data suffer some uncertainty in the early stages of decay (up to ~1 ns) and are therefore only qualitatively correct. This uncertainty is due to the short decay times involved coupled with a low density of spectral data in this region.

(31) Constant band shape is assumed or verified over the relevant time range and a peak normalization (equivalent to area normalization if spectral band shape is retained) is usually employed since decay data are rarely collected at the extreme spectral positions. Data in these regions would be required to obtain accurate area integrations. Peak normalization provides an internal test of the procedure for obtaining $\rho(\bar{\nu},t)$ in that it reveals the extent of band shape change that will affect the description embodied in eq 2. A significant band shape change will be exposed as a wavelength-dependent damping function.

(32) E. M. Kosower and H. Dodiuk, *J. Am. Chem. Soc.*, **96**, 6196 (1974).

(33) We have shown by simulation that with arbitrarily polarized excitation time-dependent emission anisotropy decay (emission wavelength independent) due to rotational movement of the dye does not affect the position or band shape of elementary time-resolved emission spectra. In addition, the influence of anisotropy on the decay kinetics (in particular, Bakhshiev eq 2) is negligible for the magnitude of the time-dependent emission anisotropy changes that were experimentally observed in these systems.

(34) M. Ottolenghi, *Acc. Chem. Res.*, **6**, 153 (1973).

(35) M. S. Walker, T. W. Bednar, and R. Lumry, *J. Chem. Phys.*, **45**, 3455 (1966).

(36) F. C. Greene, *Biochemistry*, **14**, 747 (1975).

(37) Y. H. Li, L. M. Chan, L. Tyer, R. T. Moody, C. M. Himel, and D. M. Hercules, *J. Am. Chem. Soc.*, **97**, 3118 (1975).

(38) C. J. Seliskar, Ph.D. Dissertation, Johns Hopkins University, Baltimore, Md., 1970.

(39) L. Brand, C. J. Seliskar, and D. C. Turner in "Probes of Structure and Function of Macromolecules and Membranes", Vol. 1, B. Chance, C. P. Lee, and J. K. Blasie, Ed., Academic Press, New York, N.Y., 1971, pp 17–39.

(40) R. P. DeToma and L. Brand, unpublished results.